Title

Reduced d-serine levels drive enhanced non-ionotropic NMDA receptor signaling and destabilization of dendritic spines in a mouse model for studying schizophrenia

Authors

Park, Deborah K
Petshow, Samuel
Anisimova, Margarita
et al.

Publication Date

2022-08-01

DOI

10.1016/j.nbd.2022.105772

Peer reviewed

HHS Public Access

Author manuscript

Neurobiol Dis. Author manuscript; available in PMC 2022 August 04.

Published in final edited form as:

Neurobiol Dis. 2022 August ; 170: 105772. doi:10.1016/j.nbd.2022.105772.

Reduced D-serine levels drive enhanced non-ionotropic NMDA receptor signaling and destabilization of dendritic spines in a mouse model for studying schizophrenia

Deborah K. Park[a], **Samuel Petshow**[a], **Margarita Anisimova**[a], **Eden V. Barragan**[b], **John A. Gray**[b], **Ivar S. Stein**[a], **Karen Zito**[a,*]

[a]Center for Neuroscience, Department of Neurobiology, Physiology & Behavior, University of California, Davis, CA 95618, USA

[b]Center for Neuroscience, Department of Neurology, University of California, Davis, CA 95618, USA

Abstract

Schizophrenia is a psychiatric disorder that affects over 20 million people globally. Notably, schizophrenia is associated with decreased density of dendritic spines and decreased levels of D-serine, a co-agonist required for opening of the *N*-methyl-D-aspartate receptor (NMDAR). We hypothesized that lowered D-serine levels associated with schizophrenia would enhance ion flux-independent signaling by the NMDAR, driving destabilization and loss of dendritic spines. We tested our hypothesis using the serine racemase knockout (SRKO) mouse model, which lacks the enzyme for D-serine production. We show that activity-dependent spine growth is impaired in SRKO mice, but can be acutely rescued by exogenous D-serine. Moreover, we find a significant bias of synaptic plasticity toward spine shrinkage in the SRKO mice as compared to wild-type littermates. Notably, we demonstrate that enhanced ion flux-independent signaling through the NMDAR contributes to this bias toward spine destabilization, which is exacerbated by an increase in synaptic NMDARs in hippocampal synapses of SRKO mice. Our results support a model in which lowered D-serine levels associated with schizophrenia enhance ion flux-independent NMDAR signaling and bias toward spine shrinkage and destabilization.

Keywords

Dendritic spine; Structural plasticity; NMDA receptor; Serine racemase; Schizophrenia; Two-photon glutamate uncaging

*Corresponding author. kzito@ucdavis.edu (K. Zito).

Author contributions

D.K.P., I.S.S., and K.Z. designed the study and wrote the initial draft of the manuscript. D.K.P., S.P., and M.A. performed imaging and biochemistry experiments and analysis. D.K.P., J.A.G., and E.V.B. designed and E.V.B. performed electrophysiology experiments and analysis. All authors edited the manuscript.

Declaration of Competing Interest

The authors declare no competing interests.

Appendix A. Supplementary data

Supplementary data to this article can be found online at https://doi.org/10.1016/j.nbd.2022.105772.

1. Introduction

Experience-dependent growth and long-term stabilization of dendritic spines are critical for learning and memory (Hayashi-Takagi et al., 2015). Long-term changes in spine structure and stability are tightly associated with long-term potentiation (LTP) (Hill and Zito, 2013; Matsuzaki et al., 2004) and long-term depression (LTD) (Oh et al., 2013; Zhou et al., 2004) of synaptic strength and are mediated through activation of *N*-methyl-D-aspartate receptors (NMDARs). NMDARs can signal through flux of positive ions, including Ca^{2+}, in response to binding of both glutamate and co-agonist, glycine or D-serine. In addition, NMDARs can signal in an ion flux-independent manner upon the binding of agonist or co-agonist alone (Park et al., 2022; Valbuena and Lerma, 2016). Notably, recent studies have demonstrated that glutamate binding to NMDARs in the absence of co-agonist drives LTD and spine shrinkage (Nabavi et al., 2013; Stein et al., 2015).

Dysfunctional NMDAR signaling is thought to contribute to the etiology of schizophrenia, a psychiatric disorder that affects up to 1% of the global population and is characterized by a variety of symptoms such as hallucinations and cognitive deficits (Coyle et al., 2020; Dalmau et al., 2019). These debilitating symptoms may be linked to synaptic and neuroanatomical changes in the brain, such as decreased spine and synapse densities (Konopaske et al., 2014; Onwordi et al., 2020; Radhakrishnan et al., 2021; Rosoklija et al., 2000; Sweet et al., 2009). As NMDARs mediate bidirectional structural plasticity and stabilization of spines (Hill and Zito, 2013; Oh et al., 2013; Stein et al., 2021), alterations in NMDAR function influence spine densities and impact the ability to learn and form memories (Alvarez et al., 2007; Brigman et al., 2010; Kannangara et al., 2015; Ultanir et al., 2007). Notably, individuals with schizophrenia have decreased levels of D-serine (Bendikov et al., 2007; Hashimoto et al., 2003a) and elevated levels of kynurenic acid (Plitman et al., 2017), an endogenous antagonist of the NMDAR coagonist binding site. In addition, single nucleotide polymorphisms (SNPs) in the serine racemase enzyme for D-serine production and reduced serine racemase mRNA expression in post-mortem human brain have been reported as associated with increased risk for schizophrenia (Jaffe et al., 2018; Labrie et al., 2009; Schizophrenia Working Group of the Psychiatric Genomics, 2014; Trubetskoy et al., 2022). Furthermore, there is evidence of increased D-amino acid oxidase expression in schizophrenia (Madeira et al., 2008), which similarly would contribute to lower D-serine and subsequent NMDAR hypofunction. Importantly, animal studies that mimic NMDAR hypofunction by reducing ion flux or co-agonist binding show cognitive deficits and decreased spine density (Barnes et al., 2014; Basu et al., 2009; Labrie et al., 2009; Latysheva and Raevskii, 2003; Schobel et al., 2013; Wu et al., 2016).

We hypothesized that the decreased D-serine level associated with schizophrenia promotes ion flux-independent NMDAR signaling (Nabavi et al., 2013; Stein et al., 2015), creating a bias for spine shrinkage that ultimately leads to decreased spine density. To test our hypothesis, we used a serine racemase knockout (SRKO) (Basu et al., 2009) mouse model, which lacks the enzyme required for D-serine production and exhibits decreased levels of D-serine, decreased spine densities, and cognitive deficits (Balu et al., 2013; Basu et al., 2009). We found that SRKO mice exhibit impaired activity-dependent spine growth, and that activity-dependent spine structural plasticity in SRKO animals is biased toward spine

shrinkage and destabilization. Furthermore, we observed increased numbers of synaptic NMDARs and reduced CaMKII activation at synapses of SRKO animals. Finally, we demonstrate that non-ionotropic NMDAR signaling is increased at hippocampal synapses of SRKO animals.

2. Materials and methods

2.1. Animals

SRKO (Basu et al., 2009) and GFP-M (Feng et al., 2000) mice in a C57BL/6J background were crossed to generate serine racemase knockout and wild-type littermates with GFP expressed in a subset of hippocampal pyramidal neurons. All experimental protocols were approved by the University of California Davis Institutional Animal Care and Use Committee.

2.2. Two-photon imaging and image analysis

Acute hippocampal slices were prepared from P14-21 WT and SRKO littermates of both sexes as described (Stein et al., 2021). GFP-expressing CA1 pyramidal neurons at depths of 10–50 μm were imaged using a custom two-photon microscope (Woods et al., 2011). For each neuron, image stacks (512 × 512 pixels; 0.02 μm per pixel; 1-μm z-steps) were collected from one segment of secondary or tertiary basal dendrite at 5 min intervals at 27–30 °C in recirculating artificial cerebral spinal fluid (ACSF; in mM: 127 NaCl, 25 $NaHCO_3$, 1.2 NaH_2PO_4, 2.5 KCl, 25 D-glucose, aerated with 95%O_2/5%CO_2, ~310 mOsm, pH 7.2) with 1 μM TTX, 0.1 mM Mg^{2+}, and 2 mM Ca^{2+}, unless otherwise stated. Cells were pre-incubated for at least 10 min with 10 μM D-serine or for at least 30 min with 10 μM L-689,560 (L-689), 10 μM Bay-K and 50 μM NBQX (all from Tocris), which were included as indicated. Images are maximum projections of three-dimensional image stacks after applying a median filter (3 × 3) to raw image data. Estimated spine volume was measured from background-subtracted green fluorescence using the integrated pixel intensity of a boxed region surrounding the spine head, as described (Woods et al., 2011).

2.3. Glutamate uncaging

High-frequency uncaging (HFU) consisted of 60 pulses (720 nm; 2 ms duration, 7–11 mW at the sample) at 2 Hz delivered in ACSF containing (in mM): 2 Ca^{2+}, 0.1 Mg^{2+}, 2.5 MNI-glutamate, and 0.001 TTX. The beam was parked at a point 0.5–1 μm from the spine at the position farthest from the dendrite. HFU+ stimulation consisted of 60 pulses (720 nm; 8 ms duration, 6–10 mW at the sample) at 6 Hz, delivered in ACSF containing (in mM): 10 Ca^{2+}, 0.1 Mg^{2+}, 5 MNI-glutamate, and 0.001 TTX. For experiments using HFU+ stimulation, healthy and stimulus responsive cells were selected as described (Stein et al., 2021).

2.4. Electrophysiology

Modified transverse 300 μm slices of dorsal hippocampus were prepared from P15–P19 mice anesthetized with isoflurane (Bischofberger et al., 2006), and mounted cut side down on a Leica VT1200 vibratome in ice-cold sucrose cutting buffer containing (in mM): 210 sucrose, 25 $NaHCO_3$, 2.5 KCl, 1.25 NaH_2PO_4, 7 glucose, 7 $MgCl_2$, and 0.5 $CaCl_2$. Slices

were recovered for 1 h in 32 °C ACSF solution containing (in mM): 119 NaCl, 26.2 $NaHCO_3$, 11 glucose, 2.5 KCl, 1 NaH2PO4, 2.5 $CaCl_2$, and 1.3 $MgSO_4$. Slices were perfused in ACSF at RT containing picrotoxin (0.1 mM) and TTX (0.5 μM) and saturated with 95% O_2 / 5% CO_2. mEPSCs were recorded from CA1 pyramidal neurons patched with 3–5 MΩ borosilicate pipettes filled with intracellular solution containing (in mM): 135 cesium methanesulfonate, 8 NaCl, 10 HEPES, 0.3 Na-GTP, 4 Mg-ATP, 0.3 EGTA, and 5 QX-314 (290 mOsm, pH 7.3). Cells were discarded if series resistance varied by more than 25%. Recordings were obtained with a MultiClamp 700B amplifier (Molecular Devices), filtered at 2 kHz, digitized at 10 Hz. Miniature synaptic events were analyzed using Mini Analysis software (Synaptosoft) using a threshold amplitude of 5 pA for peak detection. To generate cumulative probability plots for amplitude and inter-event time interval, events from each CA1 pyramidal neuron (>100 per cell) were pooled. The Kolmogorov-Smirnov two-sample test (KS test) was used to compare the distribution of events between WT and SRKO. Statistical comparisons were made using Graphpad Prism 8.0.

2.5. Biochemistry

Hippocampi of P20 mice of either sex were homogenized with 1% deoxycholate. For immunoprecipitation, 50 μL of Protein G Dynabeads (Invitrogen) were pre-incubated with 2.4 μg of either CaMKIIα (Leonard et al., 1998; Leonard et al., 1999; Lu et al., 2007) or mouse IgG antibody (sc-2025, Santa Cruz Biotechnology) at RT for 10 min, washed with 0.05% TBS-tween, incubated with 1000–1500 μg of protein lysate for 30 min at RT, washed four times with 0.01% TBS-triton, and then eluted. For PSD isolation, lysates were fractionated by centrifugation and sucrose gradient, and extracted with Triton X-100, as described (Dosemeci et al., 2006). Protein samples were run on a SDS-PAGE gel at 30 mA and transferred to 0.45 um PVDF membrane for 210 min at 50 V. Blots were stained for total protein with Revert 700 Total Protein Stain Kit (LICOR). Membranes were blocked with TBS Odyssey Blocking Buffer (LICOR) and incubated overnight at 4 °C with primary antibodies for GluN2B, GluN2A, GluN1, CaMKIIα (Leonard et al., 1998; Leonard et al., 1999; Lu et al., 2007), pT286 CaMKIIα (sc-12886R, Santa Cruz), synaptophysin (Sigma S5768), Cav1.2 (FP1) (Buonarati et al., 2017), or serine racemase (sc-365,217, Santa Cruz). Secondary antibody (IRDye; LICOR) incubation was for 1 h at RT and the blots scanned and analyzed using Odyssey CLx and Image Studio.

2.6. Experimental design and statistical analysis

Cells for each condition were obtained from at least 3 independent hippocampal acute slices preparations of both sexes. Data analysis was done blind to the experimental condition. All statistics were calculated across cells and performed in GraphPad Prism 8.0. Student's unpaired *t*-test, ordinary oneway ANOVA, or two-way ANOVA with Bonferroni's multiple comparisons were used, as indicated. Details on 'n' are included in the figure legends. All data are represented as mean ± standard error of the mean (SEM). Statistical significance was set at $p < 0.05$.

3. Results

3.1. Activity-induced growth of dendritic spines is impaired in SRKO mice

NMDAR-dependent long-term potentiation (LTP) of synaptic strength and associated spine growth, mediated by simultaneous binding of glutamate and co-agonist, D-serine or glycine, is an important cellular process for memory formation and maintenance of spine density. Based on the requirement for robust calcium influx during NMDAR-dependent spine growth and stabilization, we hypothesized that reduced bioavailability of D-serine observed in individuals with schizophrenia (Bendikov et al., 2007; Hashimoto et al., 2003a) would inhibit LTP-associated spine growth. Furthermore, we predicted that the reduction in D-serine levels would increase ion flux-independent NMDAR signaling, resulting in further spine destabilization that could contribute to the reduced spine density associated with the disorder (Rosoklija et al., 2000; Sweet et al., 2009).

To begin testing our hypothesis, we first examined whether spine structural plasticity is altered in a serine racemase knockout (SRKO) mouse line, which lacks the enzyme required for D-serine production and serves as an important model for studying the consequences of reduced D-serine levels, which have been associated with schizophrenia (Basu et al., 2009). To visualize spines and dendrites for monitoring activity-dependent long-term spine growth, we crossed the SRKO mouse line with the GFP-M (Feng et al., 2000) mouse line to obtain D-serine deficient mice that have sparse neuronal GFP expression in the hippocampus. Using high-frequency uncaging (HFU) of glutamate to induce long-term spine growth at single dendritic spines on basal dendrites of CA1 neurons in acute hippocampal slices, we observed a complete inhibition of long-term spine growth in SRKO mice relative to WT littermates (Fig. 1A–C; WT: 168 ± 17%; KO: 103 ± 7%). Altered long-term spine growth in the SRKO was not due to a difference in the initial volumes of target spines in the mutant animals, as baseline size of target spines did not differ between WT and SRKO (Supplemental Fig. 1A).

Notably, the lack of long-term spine growth in SRKO was rescued with acute treatment of 10 μM D-serine (Fig. 1D–F; WT: 201 ± 23%; KO: 169 ± 16%), demonstrating that the deficit in long-term spine growth is not due to chronic alterations in synaptic function in SRKO animals or a role for serine racemase independent of D-serine synthesis. Thus, aligned with the previously reported LTP deficit in these mice (Basu et al., 2009), we conclude that activity-induced spine growth is impaired in SRKO mice.

3.2. Shift toward spine destabilization in SRKO mice

Because we observed a complete block of activity-dependent spine growth in the SRKO mice, we further wondered whether the reduced D-serine levels generated abnormal conditions, beyond just reducing ion flow through NMDARs, that disrupted downstream signaling and completely inhibited all forms of spine structural plasticity. We therefore tested whether increasing or decreasing the influx of Ca^{2+} through the NMDAR would be sufficient to drive downstream signaling and spine structural plasticity in the SRKO.

We first tested whether increasing the amount of Ca^{2+} influx would overcome the impairment of activity-dependent spine growth in the SRKO. We increased the extracellular Ca^{2+} concentration to 3 mM in order to strengthen the influx of Ca^{2+} in response to HFU

stimulation, while maintaining a set amount of glutamate binding to the NMDAR. We found that HFU in 3 mM Ca^{2+} induced long-term spine growth in both WT and SRKO mice (Fig. 2A, B; WT: 187 ± 25%; KO: 193 ± 35%), demonstrating that the signaling mechanisms downstream of Ca^{2+} influx that support long-term spine growth are intact in SRKO mice.

We next tested whether decreasing the amount of Ca^{2+} influx would result in activity-dependent spine shrinkage in the SRKO. We decreased the extracellular Ca^{2+} concentration to 0.3 mM in order to weaken the influx of Ca^{2+} in response to HFU stimulation, while maintaining a set amount of glutamate binding to the NMDAR. We found that HFU in 0.3 mM Ca^{2+} induced long-term spine shrinkage in both WT and SRKO mice (Fig. 2C, D; WT: 69 ± 7%; KO: 82 ± 3%), demonstrating that the signaling mechanisms that support long-term spine shrinkage are intact in SRKO mice.

Because we found bidirectional spine structural plasticity intact in SRKO mice, we hypothesized that the disruption of activity-dependent long-term spine growth in SRKO mice that we observed in Fig. 1 was due to a bias in spine structural plasticity toward shrinkage relative to that of WT mice. We therefore predicted that a Ca^{2+} concentration that resulted in no spine structural plasticity (at the threshold between spine shrinkage and growth) in WT mice would drive spine shrinkage in the SRKO mice. Indeed, we found that HFU in 1.5 mM Ca^{2+}, which did not lead to spine structural plasticity in WT mice, resulted in spine shrinkage in SRKO mice (Fig. 2E, F; WT: 109 ± 5%; KO: 76 ± 5%). Altered long-term spine shrinkage in the SRKO was not due to a difference in initial volumes of target spines in the mutant animals, as baseline size of target spines did not differ between WT and SRKO (Supplemental Fig. 1B). Plotting all of our data together, we observed that both genotypes have similar S-shaped plasticity curves, but the SRKO plasticity curve is significantly shifted to the right (Fig. 2G), demonstrating that a wider range of Ca^{2+} levels elicit spine shrinkage in the SRKO, thus biasing spine structural plasticity toward shrinkage.

3.3. Increased synaptic NMDARs and decreased CaMKII activation in SRKO

Recent studies have established that glutamate binding to the NMDAR in the absence of co-agonist binding is sufficient to drive destabilization and shrinkage of dendritic spines (Stein et al., 2015; Stein et al., 2020; Thomazeau et al., 2020). We predicted that binding of glutamate to NMDAR in the absence of co-agonist would drive ion flux-independent NMDAR signaling and contribute to spine destabilization and shrinkage in SRKO mice. Furthermore, because adult SRKO mice exhibit elevated NMDAR expression (Balu and Coyle, 2011; Mustafa et al., 2010), we wondered if NMDARs were also elevated in hippocampus in young mice and, in combination with the reduction in D-serine levels, would contribute to even further increase in non-ionotropic NMDAR signaling. Thus, we hypothesized that the combination of reduced D-serine levels and increased expression of NMDARs available for non-ionotropic NMDAR signaling led to the observed bias for spine shrinkage in SRKO.

To investigate whether SRKO mice also have increased synaptic NMDAR expression levels at dendritic spines within the hippocampus, we isolated postsynaptic density (PSD) fractions from the hippocampi of P20 SRKO mice. We found increased levels of the obligatory NMDAR subunit GluN1 in SRKO animals relative to WT littermates, suggesting greater

number of synaptic NMDARs (Fig. 3A, B; KO: 141 ± 11%). Interestingly, we also observed increased synaptic enrichment (Fig. 3A, B; KO: 237 ± 15%) and total expression (Fig. 3C, D; KO: 122 ± 3%) of GluN2B in SRKO relative to WT. Despite the greater number of NMDARs, we expected disrupted calcium-dependent NMDAR signaling due to reduced ion flux through the NMDAR. Indeed, when we probed CaMKII-GluN2B interaction by immunoprecipitation or phosphorylation of CaMKII at the T286 autophosphorylation site, both induced by strong calcium influx and integral for LTP (Halt et al., 2012; Lee et al., 2009), we found that basal levels of CaMKII-GluN2B interaction and pT286 are both decreased in SRKO compared to WT (Fig. 3E, F; KO CaMKII-GluN2B: 68 ± 6%; KO pT286: 89 ± 1%), despite no change in CaMKII expression or enrichment levels (Fig. 3A, B; KO CaMKII expression: 112 ± 4%; KO synaptic enrichment: 114 ± 15%). In sum, our results confirm increased NMDAR content and decreased calcium-dependent NMDAR downstream signaling in hippocampal synapses of SRKO mice.

3.4. Enhanced non-ionotropic NMDAR signaling in SRKO mice

Our observations of increased number of synaptic NMDARs in mice with reduced D-serine levels support that altered structural plasticity in SRKO could be due to increased non-ionotropic NMDAR signaling driven by glutamate binding to the increased number of NMDARs in the absence of co-agonist binding. Because there is no direct means of measuring the relative amount of non-ionotropic signaling, we first set out to probe the relative contribution of non-ionotropic NMDAR signaling to spine structural plasticity between the SRKO and WT using an assay that assesses non-ionotropic NMDAR signaling levels by monitoring spine growth that is driven with calcium influx through voltage-gated calcium channels (VGCCs) (Stein et al., 2021) (Fig. 4A). These experiments are designed based on our finding that non-ionotropic NMDAR signaling is essential not only for LTD-induced spine shrinkage, but also contributes to LTP-induced spine growth (Stein et al., 2021). We hypothesized that, under conditions of robust calcium influx through VGCCs, we would observe enhanced spine growth in the SRKO due to the enhanced synaptic NMDARs driving more non-ionotropic NMDAR signaling.

To isolate non-ionotropic NMDAR signaling in SRKO mice, we used the NMDAR co-agonist site inhibitor L-689,560 (L-689) to mimic the absence of co-agonist and thus block NMDAR-mediated Ca^{2+} influx following glutamate binding. We combined this with the L-type Ca^{2+}channel agonist Bay K 8644 (Bay K) to promote Ca^{2+} influx through VGCCs. A modified HFU paradigm (HFU+) was used to induce a weak, non-saturated long-term increase in spine size in WT mice (Fig. 4B–D). Remarkably, the same HFU+ stimulation drove a robust increase in spine growth in SRKO mice (Fig. 4B–D; WT: 122 ± 4%; KO: 171 ± 11%). Altered long-term spine growth in the SRKO was not due to a difference in the initial volumes of target spines in the mutant animals, as baseline size of target spines did not differ between WT and SRKO (Supplemental Fig. 1C). The enhancement in spine growth cannot be attributed to increased AMPAR function in SRKO mice, as the amplitude of miniature excitatory postsynaptic currents (mEPSCs) was not different between WT and SRKO (Fig. 4E; WT: 10 ± 0.6 pA; KO: 9.3 ± 0.3 pA), nor can it be attributed to increased expression of synaptic voltage-gated calcium channels or AMPARs, as synaptosomal preparations showed no change in Cav1.2 or GluA1 in SRKO compared to

WT, despite the increased GluN2B levels (Fig. 4F, G; KO Cav1.2: 94 ± 4%; KO GluA1: 104 ± 5%; KO GluN2B: 124 ± 6%). We therefore interpret the greater amount of spine growth in SRKO to be indicative of a higher level of non-ionotropic NMDAR signaling.

To confirm using a different approach that increased non-ionotropic NMDAR signaling in SRKO causes a shift of spine plasticity toward shrinkage, we next used L-689 to block co-agonist binding during a weak glutamate-uncaging stimulation. We reasoned that if SRKO mice have more synaptic NMDARs and thus undergo more non-ionotropic NMDAR signaling relative to WT, a weak glutamate uncaging stimulation that fails to induce spine shrinkage in WT should be sufficient to drive shrinkage in SRKO. Indeed, while our weaker HFU stimulus (reduced pulse width of 1 ms) in the presence of L-689 and NBQX failed to induce shrinkage of dendritic spines in WT animals (Fig. 5A–C; WT 1 ms: 99 ± 2%), despite robust shrinkage observed with the control HFU 2 ms stimulus (Fig. 5A–C; WT 2 ms: 66 ± 5%), it was sufficient to drive shrinkage of dendritic spines in SRKO mice (Fig. 5A–C; SRKO 1 ms: 72 ± 4%). Altered long-term spine shrinkage in the SRKO was not due to a difference in the initial volumes of target spines in the mutant animals, as baseline size of target spines did not differ between WT and SRKO (Supplemental Fig. 1D). These combined results support our model (Fig. 5D) in which conditions of reduced D-serine levels in SRKO lead to increased synaptic NMDARs, which drive enhanced non-ionotropic NMDAR signaling, and thus create a bias toward spine shrinkage and loss.

4. Discussion

4.1. Lowered D-serine levels create a bias toward spine shrinkage

It has been widely reported that schizophrenia is associated with a reduction in dendritic spine density that is thought to contribute to cognitive deficits. As changes in spine density and gray matter volume mirror each other (Bennett, 2011), and longitudinal MRI studies of high risk individuals report normal increase in gray matter during childhood that then declines in adolescence (Job et al., 2005; Pantelis et al., 2003; Thompson et al., 2001), a time when spine pruning increases (Penzes et al., 2011), it has been suggested that excessive spine elimination, rather than a deficit in new spine outgrowth, is the potential cause of decreased spine density in schizophrenia (Glausier and Lewis, 2013).

Here, we show a disruption of long-term spine growth and a bias toward activity-induced spine shrinkage in a SRKO mouse model for studying schizophrenia, which is reported to have decreased spine density at older ages (Balu et al., 2013). Although we focus our studies on basal dendrites, we expect to observe similar results in apical dendrites, as prior studies have established that serine racemase is present in apical dendrites of CA1 pyramidal neurons (Wong et al., 2020). Our observations that deficits in long-term spine growth in the SRKO are rescued by exogenous D-serine, combined with those of others demonstrating that decreased spine density can be rescued in these mice with D-serine treatment (Balu and Coyle, 2014), support that deficits in spine plasticity and density in the SRKO are attributable to lowered D-serine levels instead of to developmental deficits or other functions of serine racemase. Indeed, although we found deficits in spine structural plasticity in the SRKO mice, it was possible to induce both spine shrinkage and growth by manipulating the strength of our stimulation, supporting that serine racemase, the enzyme that produces

D-serine and observed to interact with various synaptic structural proteins such as PSD-95 (Lin et al., 2016; Ma et al., 2014), is itself not required for structural plasticity of spines.

As glutamate binding in the absence of co-agonist to the NMDAR drives shrinkage of dendritic spines in an ion flux-independent manner (Stein et al., 2015), we proposed that reduced levels of D-serine in the SRKO mice would drive enhanced non-ionotropic NMDAR signaling, and thus would bias spine structural plasticity toward spine shrinkage, ultimately contributing to spine loss associated with schizophrenia. Notably, D-serine has been shown to promote spine stability (Lin et al., 2016). Indeed, we saw a shift in spine structural plasticity toward spine shrinkage in the SRKO mice. However, although decreased spine densities are observed in these mice at older ages (Balu et al., 2013), we did not observe decreased spine densities in the SRKO animals relative to their WT siblings at the ages used in our studies (P14–21; Supplemental Fig. 2). This result is perhaps not surprising because the age range of mice used in our study is prior to the age (P28) when serine racemase reaches maximal expression (Folorunso et al., 2021; Miya et al., 2008). Furthermore, our studies are focused before the end of the developmental period in which glycine is replaced by D-serine as the primary synaptic NMDAR co-agonist (Le Bail et al., 2015; Papouin et al., 2012); thus, we expect that we are measuring only the initial stages of disruption of spine structural plasticity, prior to detectable consequences on spine densities.

4.2. Enhanced levels and altered composition of synaptic NMDARs in SRKO mice

Our observation of increased synaptic enrichment of NMDARs relative to WT within the hippocampus of young mice is consistent with previous studies on SRKO mice showing increased expression of GluN1 (Balu and Coyle, 2011; Mustafa et al., 2010) and GluN2B (Basu et al., 2009; Wong et al., 2020). These changes in the overall number and composition of NMDARs may be a direct consequence of reduced D-serine levels, as prior studies have demonstrated the role of co-agonist binding in priming of the NMDAR for endocytosis, with D-serine specifically acting on GluN2B subunits (Ferreira et al., 2017; Nong et al., 2003). We found that the increase in synaptic NMDAR levels was associated with an increase in the magnitude of non-ionotropic signaling in SRKO, which would be expected to drive enhanced spine destabilization and shrinkage (Stein et al., 2015; Stein et al., 2021). It is also possible that the selective enhancement of GluN2B levels conferred increased non-ionotropic NMDAR signaling; however, we consider this scenario less likely, as a recent study has shown that non-ionotropic NMDAR signaling can drive LTD without any reduction in efficacy in the absence of GluN2B (Wong and Gray, 2018).

Notably, despite the enhancement of NMDAR levels at the synapse, we observed decreased CaMKII-GluN2B interaction and decreased autophosphorylation of CaMKII in SRKO mice, which we attribute to the reduced NMDAR pore opening in the conditions of reduced co-agonist D-serine, and thus lack of strong Ca^{2+} influx required for increasing both CaMKII activity and interaction with GluN2B (Goodell et al., 2017). This altered downstream CaMKII signaling likely contributes to NMDAR hypofunction in schizophrenia (Banerjee et al., 2015).

4.3. Enhanced non-ionotropic NMDAR signaling in SRKO mice

We made several observations that together support our hypothesis that there is increased ion flux-independent NMDAR signaling driving spine destabilization in the SRKO mice. First, we observed that patterns of glutamatergic activation which normally induce spine growth in WT mice instead drive spine shrinkage in SRKO. Second, we found increased NMDARs at hippocampal synapses in the SRKO mice, which, in combination with the reduced D-serine levels, is expected to bias NMDARs toward ion flux-independent signaling. Third, we showed increased ion flux-independent NMDAR signaling in SRKO animals. Finally, we observed that weak activation of non-ionotropic NMDAR signaling that fails to induce spine shrinkage in WT can drive spine shrinkage in SRKO mice, further supporting that enhanced non-ionotropic NMDAR signaling in SRKO mice drives spine destabilization and shrinkage, and would be expected to drive eventual spine elimination.

The molecular mechanisms through which ion flux-independent NMDAR signaling leads to dendritic spine shrinkage and destabilization are beginning to be elucidated. p38 mitogen-activation protein kinase (p38 MAPK), which was shown to attain its active phosphorylated state during LTD induction even in the presence of the NMDAR pore blocker MK-801 (Nabavi et al., 2013), was the first molecule confirmed to be required for spine shrinkage initiated by non-ionotropic NMDAR signaling (Stein et al., 2015). A recent study has identified several signaling components on the pathway, including neuronal nitric oxide synthase (nNOS), the interaction between nNOS and the adaptor protein NOS1AP, the kinases MK2 and CaMKII, and the actin-depolymerizing factor cofilin (Stein et al., 2020). Another study implicated mammalian target of rapamycin complex 1 (mTORC1), which is important for protein synthesis, in spine shrinkage induced by non-ionotropic NMDAR signaling (Thomazeau et al., 2020). Furthermore, studies using FRET to monitor movements of the C terminus of the NMDAR, have shown that agonist (glutamate or NMDA) binding drives the GluN1 C-tails to move away from each other, independent of NMDAR ion flux (Aow et al., 2015; Dore et al., 2015; Ferreira et al., 2017). Intriguingly, over-expression of PSD-95 is sufficient to block both agonist-induced NMDAR conformational changes and non-ionotropic NMDAR-LTD, leading to a proposal that PSD-95 plays an important role linking NMDAR conformational changes to ion flux-independent downstream signaling (Dore and Malinow, 2020).

Studies in which NMDAR channel blockers produce schizophrenia-like symptoms in healthy individuals and exacerbate them in individuals with schizophrenia helped give rise to the NMDAR hypofunction hypothesis (Javitt and Zukin, 1991; Krystal et al., 1994; Lahti et al., 2001; Newcomer et al., 1999). Due to high sensitivity of inhibitory GABAergic neurons to NMDAR blockers (Grunze et al., 1996; Homayoun and Moghaddam, 2007), and decreased expression of both interneuronal (Hashimoto et al., 2008; Hashimoto et al., 2003b; Mellios et al., 2009), and GABAergic markers (Glausier and Lewis, 2017; Gonzalez-Burgos et al., 2011; Lewis et al., 2008; Lewis et al., 1999), NMDAR hypofunction caused by reduced D-serine levels in schizophrenia may lead to disinhibition of excitatory neurons and result in glutamate spillover (Gallinat et al., 2016; Kraguljac et al., 2013; Lorrain et al., 2003; van Elst et al., 2005). Indeed, SRKO mice have been observed to have decreased PV expression and altered excitatory/inhibitory balance from GABAergic dysfunction (Jami et

al., 2020; Ploux et al., 2020; Steullet et al., 2017). This disinhibition should result in greater release of glutamate at dendritic spines that, when paired with reduced D-serine levels and increased levels of synaptic NMDARs, would increase the amount of non-ionotropic NMDAR activation even further to promote spine shrinkage (Stein et al., 2020) and decrease in spine density in the SRKO and schizophrenia (Balu et al., 2013; Rosoklija et al., 2000; Sweet et al., 2009).

Here we show that a SRKO mouse model for studying schizophrenia displays altered dendritic structural plasticity biased toward spine shrinkage and destabilization. We further report an increased number of synaptic NMDARs in the hippocampus of SRKO mice and increased ion flux-independent NMDAR signaling at hippocampal spines. Taken together, our findings support a model in which NMDAR hypofunction brought on by lack of D-serine, promotes excessive non-ionotropic NMDAR signaling that drives a bias toward spine shrinkage and likely contributes to decreased spine density associated with schizophrenia.

Supplementary Material

Refer to Web version on PubMed Central for supplementary material.

Acknowledgements

This work was supported by the NIH (R01 NS062736, R01 MH117130 T32 GM007377, T32 MH112507, T32 GM099608), an ARCS scholar award (D.K.P.), and the Deutsche Forschungsgemeinschaft Walter Benjamin project 468470832 (M.A.). We thank Joseph Coyle for the SRKO mice; Johannes Hell for CaMKIIα, GluN1, GluN2B, GluN2A, GluA1, and Cav1.2 antibodies; Julie Culp, Jennifer Jahncke, and Lorenzo Tom for support with experiments and analysis; and Joseph Coyle, Darrick Balu, Johannes Hell, and Scott Cameron for critical input.

References

Alvarez VA, Ridenour DA, Sabatini BL, 2007. Distinct structural and ionotropic roles of NMDA receptors in controlling spine and synapse stability. J. Neurosci 27, 7365–7376. [PubMed: 17626197]

Aow J, Dore K, Malinow R, 2015. Conformational signaling required for synaptic plasticity by the NMDA receptor complex. Proc. Natl. Acad. Sci. U. S. A 112, 14711–14716. [PubMed: 26553983]

Balu DT, Coyle JT, 2011. Glutamate receptor composition of the post-synaptic density is altered in genetic mouse models of NMDA receptor hypo- and hyperfunction. Brain Res. 1392, 1–7. [PubMed: 21443867]

Balu DT, Coyle JT, 2014. Chronic D-serine reverses arc expression and partially rescues dendritic abnormalities in a mouse model of NMDA receptor hypofunction. Neurochem. Int 75, 76–78. [PubMed: 24915645]

Balu DT, Li Y, Puhl MD, Benneyworth MA, Basu AC, Takagi S, Bolshakov VY, Coyle JT, 2013. Multiple risk pathways for schizophrenia converge in serine racemase knockout mice, a mouse model of NMDA receptor hypofunction. Proc. Natl. Acad. Sci. U. S. A 110, E2400–E2409. [PubMed: 23729812]

Banerjee A, Wang HY, Borgmann-Winter KE, MacDonald ML, Kaprielian H, Stucky A, Kvasic J, Egbujo C, Ray R, Talbot K, et al. , 2015. Src kinase as a mediator of convergent molecular abnormalities leading to NMDAR hypoactivity in schizophrenia. Mol. Psychiatry 20, 1091–1100. [PubMed: 25330739]

Barnes SA, Sawiak SJ, Caprioli D, Jupp B, Buonincontri G, Mar AC, Harte MK, Fletcher PC, Robbins TW, Neill JC, et al. , 2014. Impaired limbic cortico-striatal structure and sustained visual attention in a rodent model of schizophrenia. Int. J. Neuropsychopharmacol 18.

Basu AC, Tsai GE, Ma CL, Ehmsen JT, Mustafa AK, Han L, Jiang ZI, Benneyworth MA, Froimowitz MP, Lange N, et al. , 2009. Targeted disruption of serine racemase affects glutamatergic neurotransmission and behavior. Mol. Psychiatry 14, 719–727. [PubMed: 19065142]

Bendikov I, Nadri C, Amar S, Panizzutti R, De Miranda J, Wolosker H, Agam G, 2007. A CSF and postmortem brain study of D-serine metabolic parameters in schizophrenia. Schizophr. Res 90, 41–51. [PubMed: 17156977]

Bennett MR, 2011. Schizophrenia: susceptibility genes, dendritic-spine pathology and gray matter loss. Prog. Neurobiol 95, 275–300. [PubMed: 21907759]

Bischofberger J, Engel D, Li L, Geiger JR, Jonas P, 2006. Patch-clamp recording from mossy fiber terminals in hippocampal slices. Nat. Protoc 1, 2075–2081. [PubMed: 17487197]

Brigman JL, Wright T, Talani G, Prasad-Mulcare S, Jinde S, Seabold GK, Mathur P, Davis MI, Bock R, Gustin RM, et al. , 2010. Loss of GluN2B-containing NMDA receptors in CA1 hippocampus and cortex impairs long-term depression, reduces dendritic spine density, and disrupts learning. J. Neurosci 30, 4590–4600. [PubMed: 20357110]

Buonarati OR, Henderson PB, Murphy GG, Horne MC, Hell JW, 2017. Proteolytic processing of the L-type Ca (2+) channel alpha 11.2 subunit in neurons. F1000Res 6, 1166. [PubMed: 28781760]

Coyle JT, Ruzicka WB, Balu DT, 2020. Fifty years of research on schizophrenia: the ascendance of the glutamatergic synapse. Am. J. Psychiatry 177, 1119–1128. [PubMed: 33256439]

Dalmau J, Armangue T, Planaguma J, Radosevic M, Mannara F, Leypoldt F, Geis C, Lancaster E, Titulaer MJ, Rosenfeld MR, et al. , 2019. An update on anti-NMDA receptor encephalitis for neurologists and psychiatrists: mechanisms and models. Lancet Neurol. 18, 1045–1057. [PubMed: 31326280]

Dore K, Malinow R, 2020. Elevated PSD-95 blocks ion-flux independent LTD: a potential new role for PSD-95 in synaptic plasticity. Neuroscience. 456, 43–49. [PubMed: 32114099]

Dore K, Aow J, Malinow R, 2015. Agonist binding to the NMDA receptor drives movement of its cytoplasmic domain without ion flow. Proc. Natl. Acad. Sci. U. S. A 112, 14705–14710. [PubMed: 26553997]

Dosemeci A, Tao-Cheng JH, Vinade L, Jaffe H, 2006. Preparation of postsynaptic density fraction from hippocampal slices and proteomic analysis. Biochem. Biophys. Res. Commun 339, 687–694. [PubMed: 16332460]

Feng G, Mellor RH, Bernstein M, Keller-Peck C, Nguyen QT, Wallace M, Nerbonne JM, Lichtman JW, Sanes JR, 2000. Imaging neuronal subsets in transgenic mice expressing multiple spectral variants of GFP. Neuron 28, 41–51. [PubMed: 11086982]

Ferreira JS, Papouin T, Ladepeche L, Yao A, Langlais VC, Bouchet D, Dulong J, Mothet JP, Sacchi S, Pollegioni L, et al. , 2017. Co-agonists differentially tune GluN2B-NMDA receptor trafficking at hippocampal synapses. Elife 6.

Folorunso OO, Harvey TL, Brown SE, Cruz C, Shahbo E, Ajjawi I, Balu DT, 2021. Forebrain expression of serine racemase during postnatal development. Neurochem. Int 145, 104990. [PubMed: 33592203]

Gallinat J, McMahon K, Kuhn S, Schubert F, Schaefer M, 2016. Cross-sectional study of glutamate in the anterior cingulate and hippocampus in schizophrenia. Schizophr. Bull 42, 425–433. [PubMed: 26333842]

Glausier JR, Lewis DA, 2013. Dendritic spine pathology in schizophrenia. Neuroscience 251, 90–107. [PubMed: 22546337]

Glausier JR, Lewis DA, 2017. GABA and schizophrenia: where we stand and where we need to go. Schizophr. Res 181, 2–3. [PubMed: 28179064]

Gonzalez-Burgos G, Fish KN, Lewis DA, 2011. GABA neuron alterations, cortical circuit dysfunction and cognitive deficits in schizophrenia. Neural. Plast 2011, 723184. [PubMed: 21904685]

Goodell DJ, Zaegel V, Coultrap SJ, Hell JW, Bayer KU, 2017. DAPK1 mediates LTD by making CaMKII/GluN2B binding LTP specific. Cell Rep. 19, 2231–2243. [PubMed: 28614711]

Grunze HC, Rainnie DG, Hasselmo ME, Barkai E, Hearn EF, McCarley RW, Greene RW, 1996. NMDA-dependent modulation of CA1 local circuit inhibition. J. Neurosci 16, 2034–2043. [PubMed: 8604048]

Halt AR, Dallapiazza RF, Zhou Y, Stein IS, Qian H, Juntti S, Wojcik S, Brose N, Silva AJ, Hell JW, 2012. CaMKII binding to GluN2B is critical during memory consolidation. EMBO J. 31, 1203–1216. [PubMed: 22234183]

Hashimoto K, Fukushima T, Shimizu E, Komatsu N, Watanabe H, Shinoda N, Nakazato M, Kumakiri C, Okada S, Hasegawa H, et al. , 2003a. Decreased serum levels of D-serine in patients with schizophrenia: evidence in support of the N-methyl-D-aspartate receptor hypofunction hypothesis of schizophrenia. Arch. Gen. Psychiatry 60, 572–576. [PubMed: 12796220]

Hashimoto T, Volk DW, Eggan SM, Mirnics K, Pierri JN, Sun Z, Sampson AR, Lewis DA, 2003b. Gene expression deficits in a subclass of GABA neurons in the prefrontal cortex of subjects with schizophrenia. J. Neurosci 23, 6315–6326. [PubMed: 12867516]

Hashimoto T, Arion D, Unger T, Maldonado-Aviles JG, Morris HM, Volk DW, Mirnics K, Lewis DA, 2008. Alterations in GABA-related transcriptome in the dorsolateral prefrontal cortex of subjects with schizophrenia. Mol. Psychiatry 13, 147–161. [PubMed: 17471287]

Hayashi-Takagi A, Yagishita S, Nakamura M, Shirai F, Wu YI, Loshbaugh AL, Kuhlman B, Hahn KM, Kasai H, 2015. Labelling and optical erasure of synaptic memory traces in the motor cortex. Nature 525, 333–338. [PubMed: 26352471]

Hill TC, Zito K, 2013. LTP-induced long-term stabilization of individual nascent dendritic spines. J. Neurosci 33, 678–686. [PubMed: 23303946]

Homayoun H, Moghaddam B, 2007. NMDA receptor hypofunction produces opposite effects on prefrontal cortex interneurons and pyramidal neurons. J. Neurosci 27, 11496–11500. [PubMed: 17959792]

Jaffe AE, Straub RE, Shin JH, Tao R, Gao Y, Collado-Torres L, Kam-Thong T, Xi HS, Quan J, Chen Q, et al. , 2018. Developmental and genetic regulation of the human cortex transcriptome illuminate schizophrenia pathogenesis. Nat. Neurosci 21, 1117–1125. [PubMed: 30050107]

Jami SA, Cameron S, Wong JM, Daly ER, McAllister AK, Gray JA, 2020. Increased excitation-inhibition balance due to a loss of GABAergic synapses in the serine racemase knockout model of NMDA receptor hypofunction. J. Neurophysiol 126, 11–27.

Javitt DC, Zukin SR, 1991. Recent advances in the phencyclidine model of schizophrenia. Am. J. Psychiatry 148, 1301–1308. [PubMed: 1654746]

Job DE, Whalley HC, Johnstone EC, Lawrie SM, 2005. Grey matter changes over time in high risk subjects developing schizophrenia. Neuroimage 25, 1023–1030. [PubMed: 15850721]

Kannangara TS, Eadie BD, Bostrom CA, Morch K, Brocardo PS, Christie BR, 2015. GluN2A −/− mice lack bidirectional synaptic plasticity in the dentate gyrus and perform poorly on spatial pattern separation tasks. Cereb. Cortex 25, 2102–2113. [PubMed: 24554729]

Konopaske GT, Lange N, Coyle JT, Benes FM, 2014. Prefrontal cortical dendritic spine pathology in schizophrenia and bipolar disorder. JAMA Psychiatry 71, 1323–1331. [PubMed: 25271938]

Kraguljac NV, White DM, Reid MA, Lahti AC, 2013. Increased hippocampal glutamate and volumetric deficits in unmedicated patients with schizophrenia. JAMA Psychiatry 70, 1294–1302. [PubMed: 24108440]

Krystal JH, Karper LP, Seibyl JP, Freeman GK, Delaney R, Bremner JD, Heninger GR, Bowers MB Jr., Charney DS, 1994. Subanesthetic effects of the noncompetitive NMDA antagonist, ketamine, in humans. Psychotomimetic, perceptual, cognitive, and neuroendocrine responses. Arch. Gen. Psychiatry 51, 199–214. [PubMed: 8122957]

Labrie V, Fukumura R, Rastogi A, Fick LJ, Wang W, Boutros PC, Kennedy JL, Semeralul MO, Lee FH, Baker GB, et al. , 2009. Serine racemase is associated with schizophrenia susceptibility in humans and in a mouse model. Hum. Mol. Genet 18, 3227–3243. [PubMed: 19483194]

Lahti AC, Weiler MA, Tamara Michaelidis BA, Parwani A, Tamminga CA, 2001. Effects of ketamine in normal and schizophrenic volunteers. Neuropsychopharmacology 25, 455–467. [PubMed: 11557159]

Latysheva NV, Raevskii KS, 2003. Behavioral analysis of the consequences of chronic blockade of NMDA-type glutamate receptors in the early postnatal period in rats. Neurosci. Behav. Physiol 33, 123–131. [PubMed: 12669782]

Le Bail M, Martineau M, Sacchi S, Yatsenko N, Radzishevsky I, Conrod S, Ait Ouares K, Wolosker H, Pollegioni L, Billard JM, et al. , 2015. Identity of the NMDA receptor coagonist is synapse

specific and developmentally regulated in the hippocampus. Proc. Natl. Acad. Sci. U. S. A 112, E204–E213. [PubMed: 25550512]

Lee SJ, Escobedo-Lozoya Y, Szatmari EM, Yasuda R, 2009. Activation of CaMKII in single dendritic spines during long-term potentiation. Nature 458, 299–304 [PubMed: 19295602]

Leonard AS, Davare MA, Horne MC, Garner CC, Hell JW, 1998. SAP97 is associated with the alpha-amino-3-hydroxy-5-methylisoxazole-4-propionic acid receptor GluR1 subunit. J. Biol. Chem 273, 19518–19524. [PubMed: 9677374]

Leonard AS, Lim IA, Hemsworth DE, Horne MC, Hell JW, 1999. Calcium/calmodulin-dependent protein kinase II is associated with the N-methyl-D-aspartate receptor. Proc. Natl. Acad. Sci. U. S. A 96, 3239–3244. [PubMed: 10077668]

Lewis DA, Pierri JN, Volk DW, Melchitzky DS, Woo TU, 1999. Altered GABA neurotransmission and prefrontal cortical dysfunction in schizophrenia. Biol. Psychiatry 46, 616–626. [PubMed: 10472415]

Lewis DA, Hashimoto T, Morris HM, 2008. Cell and receptor type-specific alterations in markers of GABA neurotransmission in the prefrontal cortex of subjects with schizophrenia. Neurotox. Res 14, 237–248. [PubMed: 19073429]

Lin H, Jacobi AA, Anderson SA, Lynch DR, 2016. D-serine and serine racemase are associated with PSD-95 and glutamatergic synapse stability. Front. Cell. Neurosci 10, 34. [PubMed: 26941605]

Lorrain DS, Baccei CS, Bristow LJ, Anderson JJ, Varney MA, 2003. Effects of ketamine and N-methyl-D-aspartate on glutamate and dopamine release in the rat prefrontal cortex: modulation by a group II selective metabotropic glutamate receptor agonist LY379268. Neuroscience 117, 697–706. [PubMed: 12617973]

Lu Y, Allen M, Halt AR, Weisenhaus M, Dallapiazza RF, Hall DD, Usachev YM, McKnight GS, Hell JW, 2007. Age-dependent requirement of AKAP150-anchored PKA and GluR2-lacking AMPA receptors in LTP. EMBO J. 26, 4879–4890. [PubMed: 17972919]

Ma TM, Paul BD, Fu C, Hu S, Zhu H, Blackshaw S, Wolosker H, Snyder SH, 2014. Serine racemase regulated by binding to stargazin and PSD-95: potential N-methyl-D-aspartate-alpha-amino-3-hydroxy-5-methyl-4-isoxazolepropionic acid (NMDA-AMPA) glutamate neurotransmission cross-talk. J. Biol. Chem 289, 29631–29641. [PubMed: 25164819]

Madeira C, Freitas ME, Vargas-Lopes C, Wolosker H, Panizzutti R, 2008. Increased brain D-amino acid oxidase (DAAO) activity in schizophrenia. Schizophr. Res 101, 76–83. [PubMed: 18378121]

Matsuzaki M, Honkura N, Ellis-Davies GC, Kasai H, 2004. Structural basis of long-term potentiation in single dendritic spines. Nature 429, 761–766. [PubMed: 15190253]

Mellios N, Huang HS, Baker SP, Galdzicka M, Ginns E, Akbarian S, 2009. Molecular determinants of dysregulated GABAergic gene expression in the prefrontal cortex of subjects with schizophrenia. Biol. Psychiatry 65, 1006–1014. [PubMed: 19121517]

Miya K, Inoue R, Takata Y, Abe M, Natsume R, Sakimura K, Hongou K, Miyawaki T, Mori H, 2008. Serine racemase is predominantly localized in neurons in mouse brain. J. Comp. Neurol 510, 641–654. [PubMed: 18698599]

Mustafa AK, Ahmad AS, Zeynalov E, Gazi SK, Sikka G, Ehmsen JT, Barrow RK, Coyle JT, Snyder SH, Dore S, 2010. Serine racemase deletion protects against cerebral ischemia and excitotoxicity. J. Neurosci 30, 1413–1416. [PubMed: 20107067]

Nabavi S, Kessels HW, Alfonso S, Aow J, Fox R, Malinow R, 2013. Metabotropic NMDA receptor function is required for NMDA receptor-dependent long-term depression. Proc. Natl. Acad. Sci. U. S. A 110, 4027–4032. [PubMed: 23431133]

Newcomer JW, Farber NB, Jevtovic-Todorovic V, Selke G, Melson AK, Hershey T, Craft S, Olney JW, 1999. Ketamine-induced NMDA receptor hypofunction as a model of memory impairment and psychosis. Neuropsychopharmacology 20, 106–118. [PubMed: 9885791]

Nong Y, Huang YQ, Ju W, Kalia LV, Ahmadian G, Wang YT, Salter MW, 2003. Glycine binding primes NMDA receptor internalization. Nature 422, 302–307. [PubMed: 12646920]

Oh WC, Hill TC, Zito K, 2013. Synapse-specific and size-dependent mechanisms of spine structural plasticity accompanying synaptic weakening. Proc. Natl. Acad. Sci. U. S. A 110, E305–E312. [PubMed: 23269840]

Onwordi EC, Halff EF, Whitehurst T, Mansur A, Cotel MC, Wells L, Creeney H, Bonsall D, Rogdaki M, Shatalina E, et al. , 2020. Synaptic density marker SV2A is reduced in schizophrenia patients and unaffected by antipsychotics in rats. Nat. Commun 11, 246. [PubMed: 31937764]

Pantelis C, Velakoulis D, McGorry PD, Wood SJ, Suckling J, Phillips LJ, Yung AR, Bullmore ET, Brewer W, Soulsby B, et al. , 2003. Neuroanatomical abnormalities before and after onset of psychosis: a cross-sectional and longitudinal MRI comparison. Lancet 361, 281–288. [PubMed: 12559861]

Papouin T, Ladepeche L, Ruel J, Sacchi S, Labasque M, Hanini M, Groc L, Pollegioni L, Mothet JP, Oliet SH, 2012. Synaptic and extrasynaptic NMDA receptors are gated by different endogenous coagonists. Cell 150, 633–646. [PubMed: 22863013]

Park DK, Stein IS, Zito K, 2022. Ion flux-independent NMDA receptor signaling. Neuropharmacology 210, 109019. [PubMed: 35278420]

Penzes P, Cahill ME, Jones KA, VanLeeuwen JE, Woolfrey KM, 2011. Dendritic spine pathology in neuropsychiatric disorders. Nat. Neurosci 14, 285–293. [PubMed: 21346746]

Plitman E, Iwata Y, Caravaggio F, Nakajima S, Chung JK, Gerretsen P, Kim J, Takeuchi H, Chakravarty MM, Remington G, et al. , 2017. Kynurenic acid in schizophrenia: a systematic review and Meta-analysis. Schizophr. Bull 43, 764–777. [PubMed: 28187219]

Ploux E, Bouet V, Radzishevsky I, Wolosker H, Freret T, Billard JM, 2020. Serine racemase deletion affects the excitatory/inhibitory balance of the hippocampal CA1 network. Int. J. Mol. Sci 21.

Radhakrishnan R, Skosnik PD, Ranganathan M, Naganawa M, Toyonaga T, Finnema S, Hillmer AT, Esterlis I, Huang Y, Nabulsi N, et al. , 2021. In vivo evidence of lower synaptic vesicle density in schizophrenia. Mol. Psychiatry 26, 7690–7698. [PubMed: 34135473]

Rosoklija G, Toomayan G, Ellis SP, Keilp J, Mann JJ, Latov N, Hays AP, Dwork AJ, 2000. Structural abnormalities of subicular dendrites in subjects with schizophrenia and mood disorders: preliminary findings. Arch. Gen. Psychiatry 57, 349–356. [PubMed: 10768696]

Schizophrenia Working Group of the Psychiatric Genomics, C, 2014. Biological insights from 108 schizophrenia-associated genetic loci. Nature 511, 421–427. [PubMed: 25056061]

Schobel SA, Chaudhury NH, Khan UA, Paniagua B, Styner MA, Asllani I, Inbar BP, Corcoran CM, Lieberman JA, Moore H, et al. , 2013. Imaging patients with psychosis and a mouse model establishes a spreading pattern of hippocampal dysfunction and implicates glutamate as a driver. Neuron 78, 81–93. [PubMed: 23583108]

Stein IS, Gray JA, Zito K, 2015. Non-ionotropic NMDA receptor signaling drives activity-induced dendritic spine shrinkage. J. Neurosci 35, 12303–12308. [PubMed: 26338340]

Stein IS, Park DK, Flores JC, Jahncke JN, Zito K, 2020. Molecular mechanisms of non-ionotropic NMDA receptor signaling in dendritic spine shrinkage. J. Neurosci 40, 3741–3750. [PubMed: 32321746]

Stein IS, Park DK, Claiborne N, Zito K, 2021. Non-ionotropic NMDA receptor signaling gates bidirectional structural plasticity of dendritic spines. Cell Rep. 34, 108664. [PubMed: 33503425]

Steullet P, Cabungcal JH, Coyle J, Didriksen M, Gill K, Grace AA, Hensch TK, LaMantia AS, Lindemann L, Maynard TM, et al. , 2017. Oxidative stress-driven parvalbumin interneuron impairment as a common mechanism in models of schizophrenia. Mol. Psychiatry 22, 936–943. [PubMed: 28322275]

Sweet RA, Henteleff RA, Zhang W, Sampson AR, Lewis DA, 2009. Reduced dendritic spine density in auditory cortex of subjects with schizophrenia. Neuropsychopharmacology 34, 374–389. [PubMed: 18463626]

Thomazeau A, Bosch M, Essayan-Perez S, Barnes SA, De Jesus-Cortes H, Bear MF, 2020. Dissociation of functional and structural plasticity of dendritic spines during NMDAR and mGluR-dependent long-term synaptic depression in wild-type and fragile X model mice. Mol. Psychiatry 26, 4652–4669. [PubMed: 32606374]

Thompson PM, Vidal C, Giedd JN, Gochman P, Blumenthal J, Nicolson R, Toga AW, Rapoport JL, 2001. Mapping adolescent brain change reveals dynamic wave of accelerated gray matter loss in very early-onset schizophrenia. Proc. Natl. Acad. Sci. U. S. A 98, 11650–11655. [PubMed: 11573002]

Trubetskoy V, Pardinas AF, Qi T, Panagiotaropoulou G, Awasthi S, Bigdeli TB, Bryois J, Chen CY, Dennison CA, Hall LS, et al. , 2022. Mapping genomic loci implicates genes and synaptic biology in schizophrenia. Nature 604, 502–508. [PubMed: 35396580]

Ultanir SK, Kim JE, Hall BJ, Deerinck T, Ellisman M, Ghosh A, 2007. Regulation of spine morphology and spine density by NMDA receptor signaling in vivo. Proc. Natl. Acad. Sci. U. S. A 104, 19553–19558. [PubMed: 18048342]

Valbuena S, Lerma J, 2016. Non-canonical signaling, the hidden life of ligand-gated ion channels. Neuron 92, 316–329 [PubMed: 27764665]

van Elst LT, Valerius G, Buchert M, Thiel T, Rusch N, Bubl E, Hennig J, Ebert D, Olbrich HM, 2005. Increased prefrontal and hippocampal glutamate concentration in schizophrenia: evidence from a magnetic resonance spectroscopy study. Biol. Psychiatry 58, 724–730. [PubMed: 16018980]

Wong JM, Gray JA, 2018. Long-term depression is independent of GluN2 subunit composition. J. Neurosci 38, 4462–4470. [PubMed: 29593052]

Wong JM, Folorunso OO, Barragan EV, Berciu C, Harvey TL, Coyle JT, Balu DT, Gray JA, 2020. Postsynaptic serine racemase regulates NMDA receptor function. J. Neurosci 40, 9564–9575. [PubMed: 33158959]

Woods GF, Oh WC, Boudewyn LC, Mikula SK, Zito K, 2011. Loss of PSD-95 enrichment is not a prerequisite for spine retraction. J. Neurosci 31, 12129–12138. [PubMed: 21865455]

Wu H, Wang X, Gao Y, Lin F, Song T, Zou Y, Xu L, Lei H, 2016. NMDA receptor antagonism by repetitive MK801 administration induces schizophrenia-like structural changes in the rat brain as revealed by voxel-based morphometry and diffusion tensor imaging. Neuroscience 322, 221–233. [PubMed: 26917273]

Zhou Q, Homma KJ, Poo MM, 2004. Shrinkage of dendritic spines associated with long-term depression of hippocampal synapses. Neuron 44, 749–757. [PubMed: 15572107]

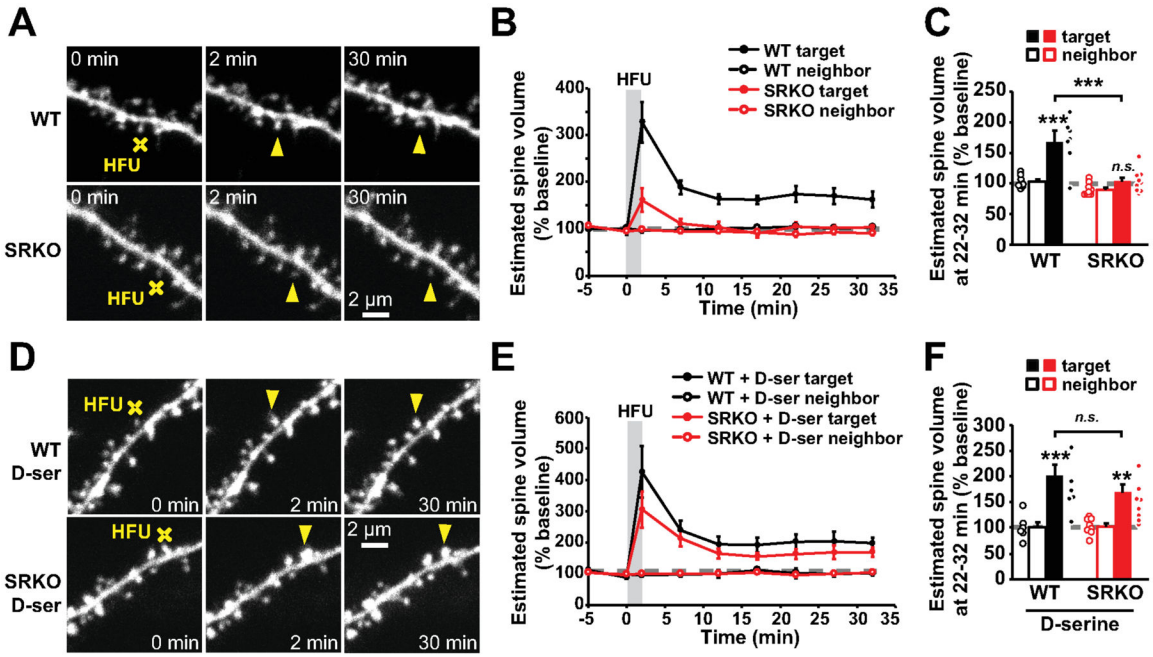

Fig. 1. LTP-associated growth of dendritic spines is impaired in SRKO mice.

A, D) Images of basal dendrites of CA1 pyramidal neurons in acute hippocampal slices from WT and SRKO mice (P14–21). Individual spines (yellow arrowhead) were stimulated with high frequency glutamate uncaging (HFU, yellow crosshair) during vehicle condition or in the presence of D-serine (10 µM). **B, C)** HFU leads to long-term spine growth in WT (black filled circles/bar; $n = 7$ cells/7 mice) but not in SRKO (red filled circles/bar; $n = 9$ cells/8 mice; $p > 0.99$) relative to baseline. **E, F)** Addition of D-serine rescues HFU-induced long-term spine growth (red filled circles/bar; $n = 8$ cells/7 mice) to levels comparable to those in WT (black filled circles/bar; $n = 6$ cells/5 mice; $p = 0.55$). Data are represented as mean +/− SEM. Two-way ANOVA with Bonferroni post hoc multiple comparison test. *$p < 0.05$; **$p < 0.01$; ***$p < 0.001$.

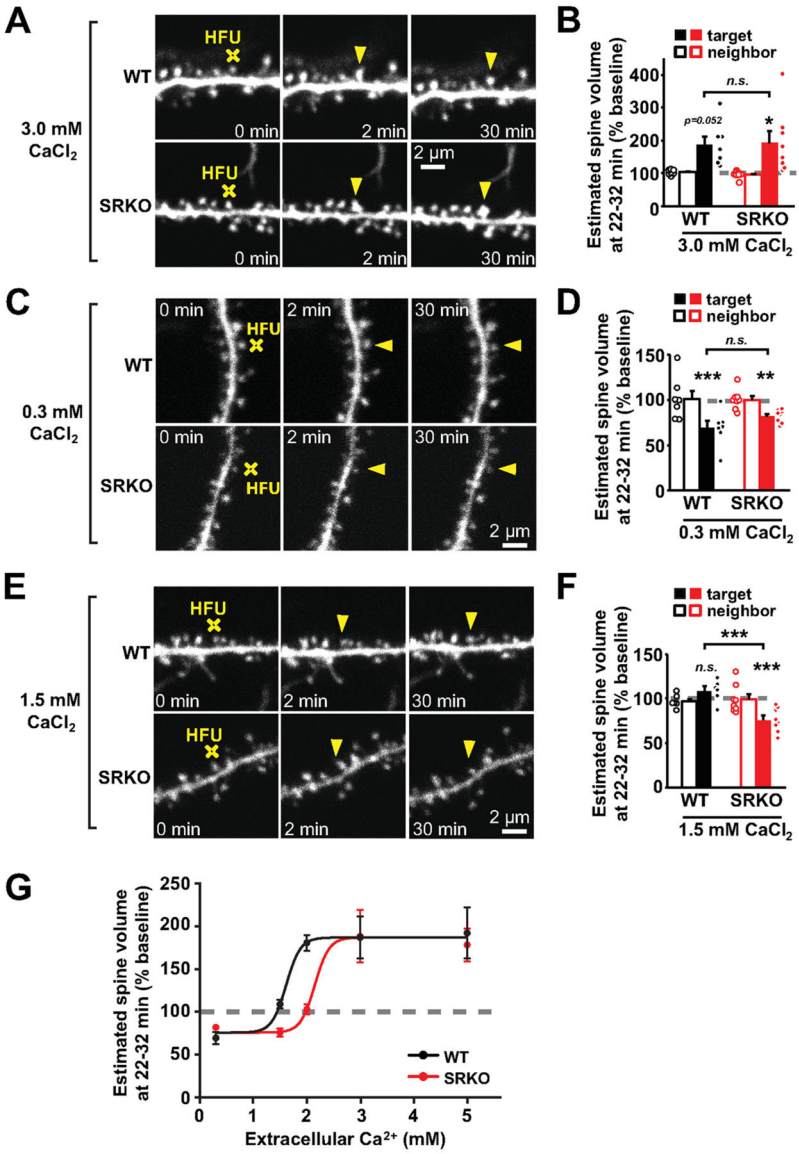

Fig. 2. Structural plasticity is shifted to favor spine shrinkage in SRKO mice.

A,C,E) Images of basal dendrites of CA1 pyramidal neurons from WT and SRKO mice (P14–21). Individual spines (yellow arrowhead) were stimulated with HFU (yellow crosshair) in ACSF with different $CaCl_2$ concentrations. **B)** HFU in ASCF containing 3 mM $CaCl_2$ drives long-term spine growth in WT (black filled circles/bar; n = 7 cells/5 mice) and SRKO (red filled circles/bar; n = 9 cells/3 mice) relative to baseline. **D)** HFU in ACSF containing 0.3 mM $CaCl_2$ drives long-term spine shrinkage in both WT (black filled circles/bar; n = 7 cells/4 mice) and SRKO (red filled circles/bar; n = 8 cells/5 mice) relative to baseline. **F)** HFU in ACSF containing 1.5 mM $CaCl_2$ does not drive any long-term spine volume change in WT (black filled circles/bar; n = 6 cells/6 mice) but drives shrinkage in SRKO (red filled circles/bar; n = 8 cells/5 mice) relative to baseline. **G)** Summary of data from Fig. 1A–B and 2A–F. Structural plasticity curve of SRKO mice is shifted to the right ($p < 0.001$; $F = 8.1$; ordinary oneway ANOVA), demonstrating a bias for spine shrinkage.

Data are represented as mean +/− SEM. Unless otherwise noted, two-way ANOVA with Bonferroni post hoc multiple comparisons test. *p <0.05; **p < 0.01; ***p < 0.001.

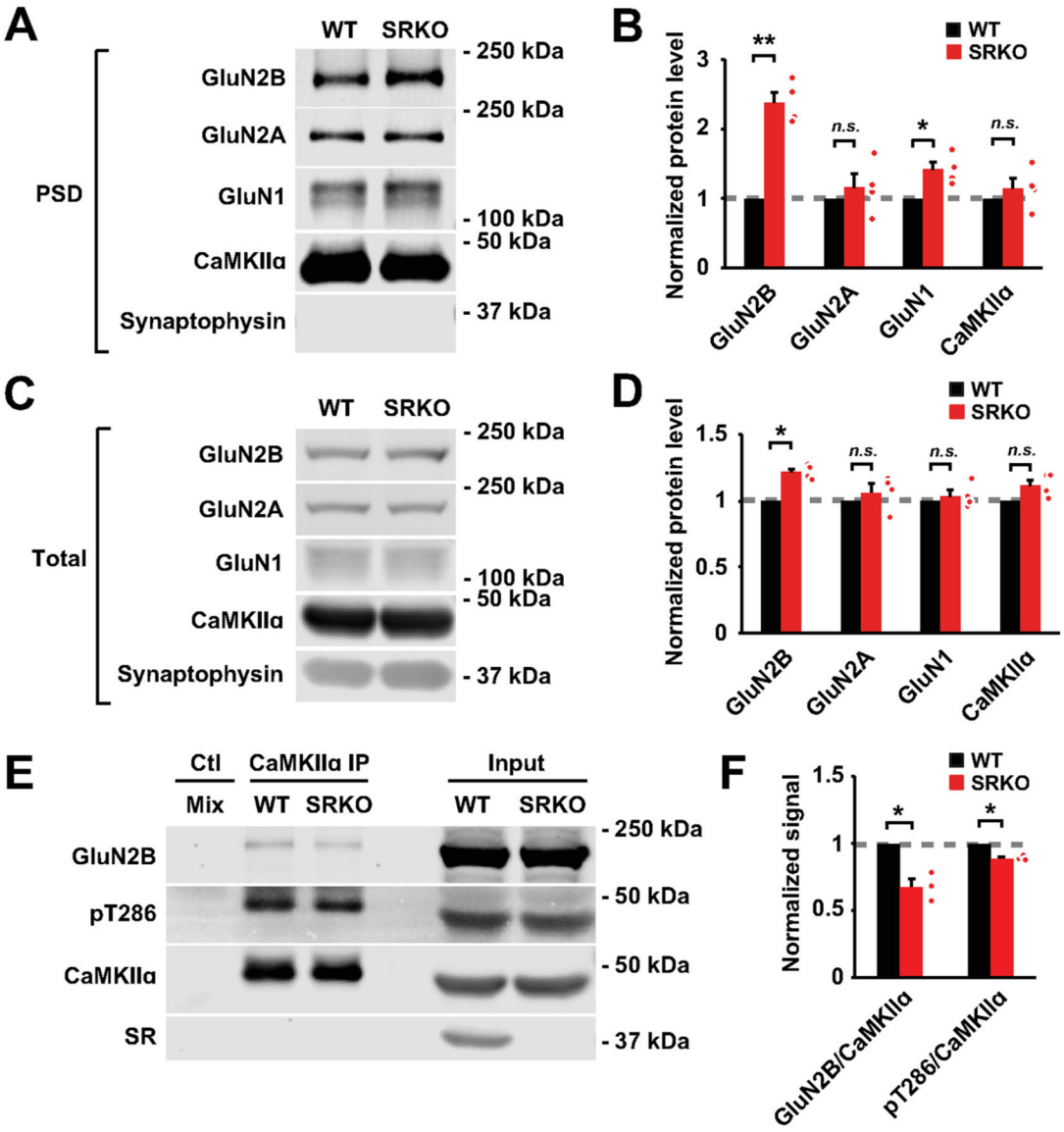

Fig. 3. Increased synaptic NMDARs and decreased CaMKII activation in SRKO mice.

A, B) PSD signals from P20 SRKO hippocampi (n = 12 mice/4 preps) show increased levels of synaptic GluN2B (p = 0.003) and GluN1 (p = 0.033) relative to WT. No change in levels of GluN2A (p = 0.49) or CaMKII (p = 0.41) was observed. **C, D)** Total homogenate (n = 4 mice/ 4 preps) signal shows increased levels of GluN2B (p = 0.004) relative to WT. No change in levels of GluN2A (p = 0.41), GluN1 (p = 0.50), or CaMKII (p = 0.074) were observed. **E, F)** Immuno-precipitation of CaMKII from P20 SRKO hippocampi (n = 3 mice/3 preps) shows decreased CaMKII-GluN2B interaction (p = 0.034) and decreased pT286 levels of CaMKII (p = 0.010) relative to WT. Data are represented as mean +/− SEM. Student's unpaired t-test. *p < 0.05; **p < 0.01; ***p < 0.001.

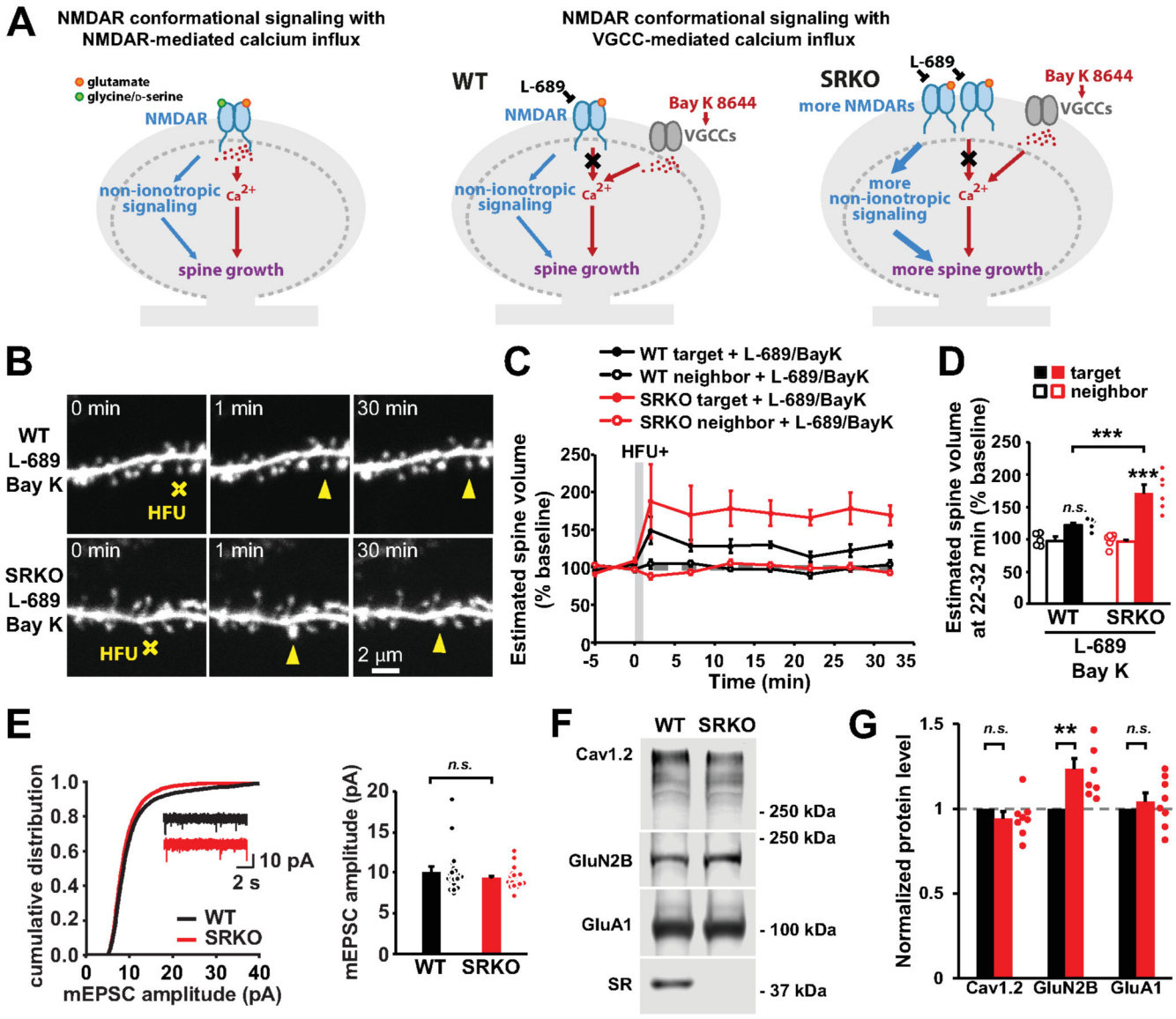

Fig. 4. Enhanced non-ionotropic NMDAR signaling in SRKO mice.

A) Left: Schematic of the signaling requirements for long-term spine growth, which include non-ionotropic NMDAR signaling and NMDAR-mediated Ca^{2+} influx. Right: Experimental design for assessing levels of non-ionotropic NMDAR signaling in WT versus SRKO mice and predicted outcomes. **B)** Images of dendrites before and after HFU+ stimulation (yellow crosshair) at individual spines (yellow arrowhead) in the presence of L-689 (10 µM), an NMDAR co-agonist site inhibitor used to block Ca^{2+} influx through NMDARs, and Bay K (10 µM) to promote Ca^{2+} influx through VGCCs. **C, D)** Although HFU+ stimulation in the presence of L-689 and BayK drives only a trend toward long-term spine growth in WT (black filled circles/bar; $n = 5$ cells/5 mice; $p = 0.2$), it leads to long-term spine growth in SRKO (red filled circles/bar; n = 6 cells/4 mice) relative to baseline. The magnitude of long-term spine growth is larger in SRKO than WT. **E)** Amplitude of mEPSCs of P15–19 CA1 pyramidal neurons is unaltered in SRKO (WT: black line/bar; $n = 20$ cells/3 mice;

SRKO red line/bar: $n = 17$ cells/3 mice; $p = 0.26$). **F, G)** Synaptosomal signal from P20 SRKO (red bars) hippocampi shows no change in GluA1 ($p = 0.22$) or Cav1.2 ($p = 0.10$) from WT (black bars), despite increased GluN2B relative to WT (n = 7 preps/21 mice). Student's unpaired t-test. Data are represented as mean +/− SEM. Unless otherwise noted, two-way ANOVA with Bonferroni post hoc multiple comparisons test. *p < 0.05; **p < 0.01; ***p < 0.001.

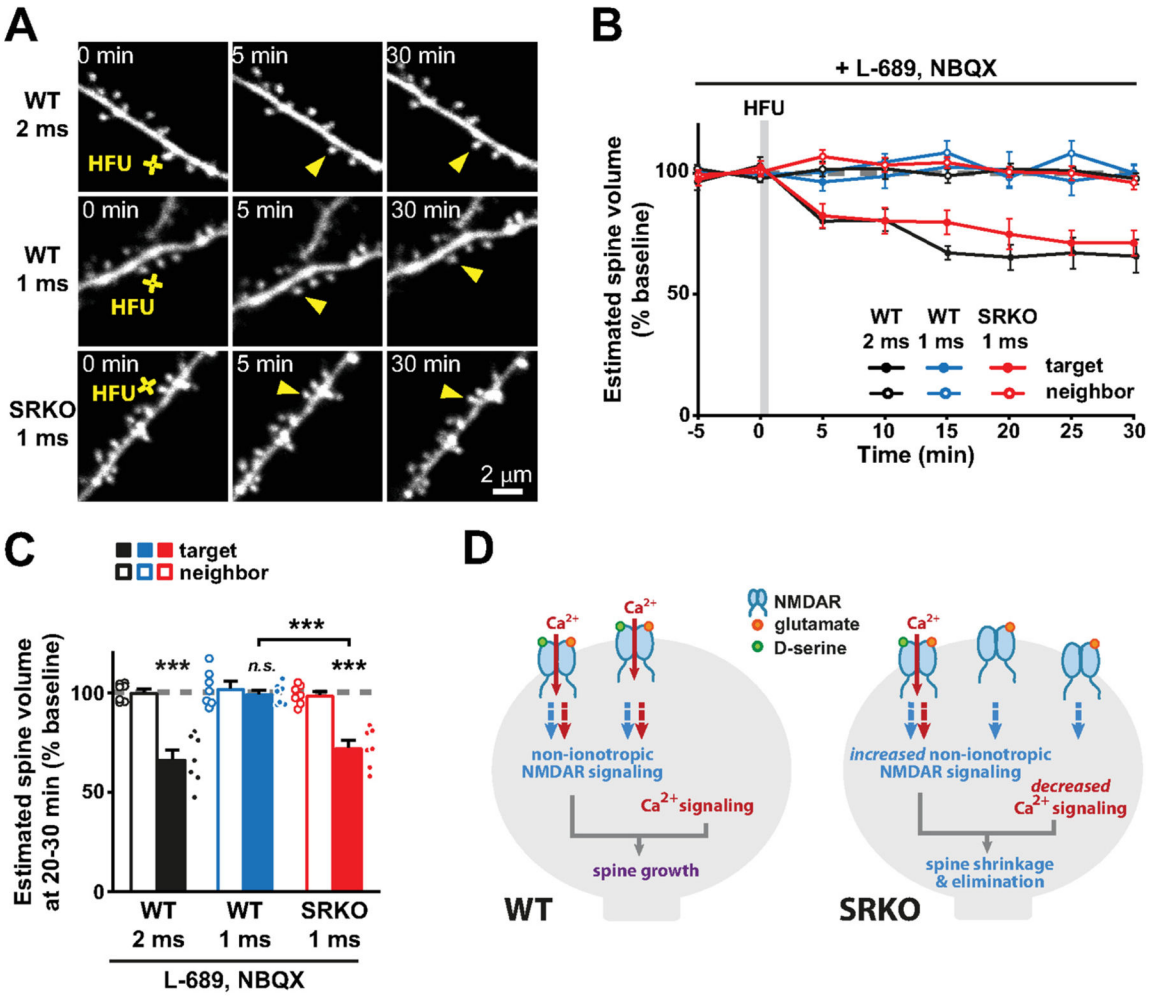

Fig. 5. Shift of plasticity toward spine shrinkage in SRKO mice.

A) Images of basal dendrites of CA1 pyramidal neurons from P14–21 WT and SRKO mice. Individual spines (yellow arrowhead) were stimulated with HFU (yellow crosshair) in the presence of L-689 (10 µM) and NBQX (50 µM) for 1 or 2 ms. **B, C)** HFU in L-689 with 2 ms pulse duration (black filled circles/bar; n = 7 cells/5 mice) leads to shrinkage of WT target spines, but not HFU in L-689 with 1 ms pulse duration (blue filled circles/bar; n = 7 cells/5 mice; $p > 0.99$) relative to baseline. In contrast, HFU in L-689 with 1 ms pulse duration (red filled circles/bar; n = 7 cells/6 mice) is sufficient to drive spine shrinkage in SRKO mice relative to baseline. Neighboring spines were unchanged in all conditions (open circles/bars). Data are represented as mean +/− SEM. Two-way ANOVA with Bonferroni post hoc multiple comparisons test. *$p < 0.05$; **$p < 0.01$; ***$p < 0.001$ **D)** Proposed model. Binding of glutamate and D-serine leads to both non-ionotropic NMDAR signaling and calcium influx required for activity-induced long-term spine growth. In contrast, increased NMDAR levels and reduced levels of D-serine in the SRKO mouse model for studying schizophrenia results in glutamate binding alone to more NMDARs in the absence of D-serine that results in strong non-ionotropic NMDAR activation with small calcium influx, promotes spine shrinkage and destabilization.